

Correlated Trends of Coexisting Magnetism and Superconductivity in Optimally Electron-Doped Oxypnictides

S. Sanna,^{1,*} P. Carretta,¹ P. Bonfà,¹ G. Prando,^{1,2} G. Allodi,³ R. De Renzi,³ T. Shiroka,^{4,5}
G. Lamura,⁶ A. Martinelli,⁷ and M. Putti⁶

¹Dipartimento di Fisica “A. Volta” and Unità CNISM di Pavia, I-27100 Pavia, Italy

²Dipartimento di Fisica “E. Amaldi”, Università di Roma3-CNISM, I-00146 Roma, Italy

³Dipartimento di Fisica and Unità CNISM di Parma, I-43124 Parma, Italy

⁴Laboratorium für Festkörperphysik, ETH-Hönggerberg, CH-8093 Zürich, Switzerland

⁵Paul Scherrer Institut, CH-5232 Villigen PSI, Switzerland

⁶CNR-SPIN and Università di Genova, via Dodecaneso 33, I-16146 Genova, Italy

⁷CNR-SPIN Corso Perrone 24, I-16146 Genova, Italy

(Received 12 August 2011; published 22 November 2011)

We report on the recovery of the short-range static magnetic order and on the concomitant degradation of the superconducting state in optimally F-doped $\text{SmFe}_{1-x}\text{Ru}_x\text{AsO}_{0.85}\text{F}_{0.15}$ for $0.1 \leq x \leq 0.5$. The two reduced order parameters coexist within nanometer-size domains in the FeAs layers and eventually disappear around a common critical threshold $x_c \sim 0.6$. Superconductivity and magnetism are shown to be closely related to two *distinct* well-defined local electronic environments of the FeAs layers. The two transition temperatures, controlled by the isoelectronic and diamagnetic Ru substitution, scale with the volume fraction of the corresponding environments. This fact indicates that superconductivity is assisted by magnetic fluctuations, which are frozen whenever a short-range static order appears, and totally vanish above the magnetic dilution threshold x_c .

DOI: 10.1103/PhysRevLett.107.227003

PACS numbers: 74.70.Xa, 74.62.Dh, 76.60.-k, 76.75.+i

The appearance of high- T_c superconductivity (SC) close to the disruption of static magnetic (M) order is a general feature of the Fe-based superconductors either as a function of doping or external pressure. In the REFeAsO family (RE1111) it is found that SC and M strongly compete and hardly coexist simultaneously [1,2], apart for RE = Sm and Ce [3,4] within a small doping range where both order parameters are depressed. Coexistence implies short-range magnetic order, that is detected only by local probes such as muon-spin rotation (μSR) [4] or nuclear quadrupole resonance (NQR) [5], since it eludes long coherence probes such as neutron powder diffraction [6]. The competition between the superconducting and magnetic ground states must be reconciled with the prevailing models of pairing mediated by spin fluctuations [7]. These models are seemingly in contradiction with the evidence that the two mutually excluding orders coexist *only* when phase separation occurs.

Here we show, by means of μSR and ^{75}As NQR, that magnetism is surprisingly still at play in optimally F-doped $\text{SmFe}_{1-x}\text{Ru}_x\text{AsO}_{0.85}\text{F}_{0.15}$. The isoelectronic Fe:Ru substitution is found to deteriorate the superconducting state in optimally electron-doped $\text{SmFeAsO}_{0.85}\text{F}_{0.15}$ samples and simultaneously to recover static magnetism within the FeAs layers, for $0.1 \leq x \leq 0.5$. This is accompanied by a local electronic rearrangement within the FeAs layers. When Ru doping approaches the critical threshold $x_c = 0.6$, corresponding to percolation of a magnetic square lattice with nearest neighbor (NN) and next-nearest neighbor hopping, both magnetism and SC vanish.

The investigated polycrystalline $\text{SmFe}_{1-x}\text{Ru}_x\text{AsO}_{0.85}\text{F}_{0.15}$ samples are the same as those of Ref. [8]. From ^{19}F nuclear magnetic resonance the relative fluorine content was found to be constant within $\Delta \approx 0.01$ in the whole set of samples investigated. To investigate the bulk character of the superconducting state we carried out transverse field (TF)- μSR measurements, where a sample is field cooled (FC) in a magnetic field larger than the lower superconducting critical field H_{c1} , applied perpendicular to the initial muon-spin direction ($\mathbf{H} \perp \mathbf{S}_\mu$). A flux line lattice is thus generated below T_c and the muon-spin precessions around the local field, B_μ , display a diamagnetic shift $B_\mu = \mu_0 H(1 + N_e \chi)$, with $\chi < 0$ and N_e an effective demagnetization factor. For samples with $x < 0.1$ the time evolution of the full TF- μSR asymmetry is fitted to a single SC component as $\mathcal{A}_{\text{TF}}(t) = a_{\text{TF}} e^{-\sigma_{\text{TF}}^2 t^2 / 2} \cos(\gamma B_\mu t)$, where a_{TF} is the amplitude, $\gamma = 8514 \mu\text{s}^{-1}/\text{T}$ is the muon gyromagnetic ratio and σ_{TF} the time decay of the precession. This fit holds over the entire T range (not shown) as expected in a bulk superconductor. The shift of B_μ with respect to the applied field is displayed vs temperature in Fig. 1 (symbols) for $x = 0.05$, together with the rescaled susceptibility (solid curve).

By contrast, for $x \geq 0.1$ the muon relaxation (not shown) becomes extremely fast already above the superconducting T_c . In polycrystals this is the signature of magnetic order taking place at $T_M > T_c$ [9]. A coexisting flux line lattice is hidden by the large magnetic damping, preventing its investigation by TF μSR . We characterized

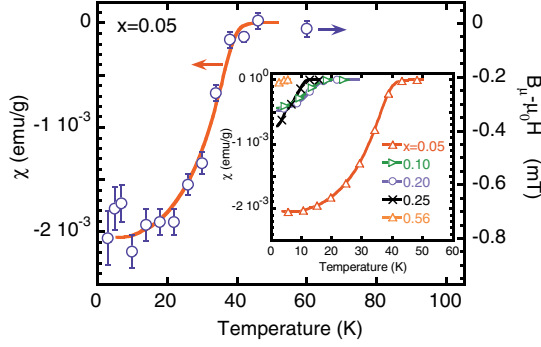


FIG. 1 (color online). Muon diamagnetic shift (TF, $\mu_0 H = 20$ mT, \circ) and zero field cooled (ZFC) SQUID susceptibility ($\mu_0 H = 0.5$ mT, solid curve) for $x = 0.05$. Inset: ZFC SQUID susceptibility $\chi(T)$ of representative $\text{SmFe}_{1-x}\text{Ru}_x\text{AsO}_{0.85}\text{F}_{0.15}$ samples ($\mu_0 H = 0.5$ mT). No relevant differences are found from FC measurements (not shown).

the superconducting response by dc magnetic susceptibility $\chi(T)$ (inset of Fig. 1), measured by a superconducting quantum interference device (SQUID). Comparison with the bulk case, $x = 0.05$, allows us to roughly estimate the SC volume fraction of the other samples, which becomes absolutely marginal above $x = 0.5$, confirming previous reports [8]. The shielding response is instead observable, but already much weaker for all samples with a reduced T_c , at odds with the behavior of analogous Nd-1111 and La-1111 Ru-doped samples [10,11], suggesting that superconductivity is not a homogeneous bulk phenomenon in $\text{SmFe}_{1-x}\text{Ru}_x\text{AsO}_{0.85}\text{F}_{0.15}$ for $x \geq 0.1$.

We now turn to zero-field (ZF)- μ SR results, sensitive to short-range magnetic order, owing to the short-range muon-spin coupling with the electronic moments. The time evolution of the (ZF)- μ SR asymmetry is displayed in the inset of Fig. 2 for $x = 0.20$ at three representative temperatures. Below a mean transition temperature $T_M \approx 30$ K the muon asymmetry is $\mathcal{A}_{\text{ZF}}(t) = a_{\text{ZF}}(w_T e^{-\sigma_T^2 t^2/2} + w_L e^{-\lambda_L t})$ displaying both a fast σ_T and a slow λ_L decay, where a_{ZF} is the high T value and $w_T + w_L = 1$. The two components reflect the orientation of the internal field with respect to the initial muon spin \mathbf{S}_μ (transverse, $\mathbf{B}_i \perp \mathbf{S}_\mu$, weight $w_T \leq 2/3$, and longitudinal, weight w_L , $\mathbf{B}_i \parallel \mathbf{S}_\mu$ plus, possibly, a fraction with vanishing internal fields). The very fast transverse relaxation ($\sigma_T \approx 30 \mu\text{s}^{-1}$) represents the signature of a sizeable distribution of internal fields \mathbf{B}_i with standard deviation $\Delta B_\mu = \sigma_T/\gamma = (\bar{B}_i^2)^{1/2}$ reaching 45 mT at low T (Fig. 2). This is a typical Fe dipolar field value at the muon site in F-doped 1111 close to a M -SC crossover [3,4]. The transverse component is overdamped down to 1.5 K (no asymmetry oscillations in Fig. 2, inset) and its fast relaxation is partially quenched in fields of order $\bar{B}_i \approx 50$ mT applied along the initial muon-spin direction (not shown), as expected for a static \mathbf{B}_i . Therefore the overdamped muon-spin precessions are due to inhomogeneous magnetic short-range order [4].

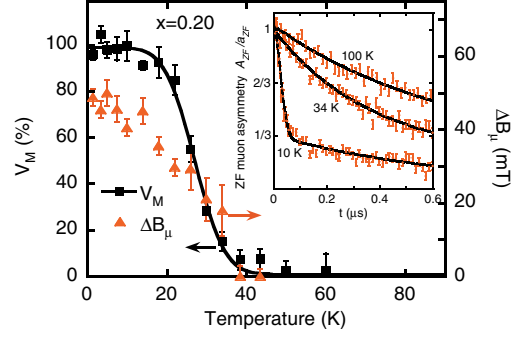


FIG. 2 (color online). Fraction of sample volume V_M (\blacksquare) where muons detect an internal magnetic field and its width ΔB_μ (\blacktriangle) vs T , for $\text{SmFe}_{1-x}\text{Ru}_x\text{AsO}_{0.85}\text{F}_{0.15}$ with $x = 0.2$. Inset: time dependence of the normalized ZF muon asymmetry, with best fits, at $T > T_M$, $T \lesssim T_M$ and $T \ll T_M$.

The fraction of the sample volume where muons experience a net field \mathbf{B}_i is calculated as $V_M = 3w_T/2 = 3(1 - w_L)/2$ [4]. Its dependence on temperature is shown in Fig. 2 for $x = 0.20$. It is noteworthy that V_M is 100% already below 20 K; i.e., internal fields develop throughout the whole sample well above the ordering temperature of the Sm sublattice ($T_N^{\text{Sm}} \approx 5$ K) [3,12] confirming that the observed magnetic order comes from the FeAs layers. In summary, since in all samples with $x \geq 0.10$ every muon detects a local magnetic field, every muon site must still be extremely close to some ordered magnetic moment. On the other hand in the same samples SQUID susceptibility detects a non-negligible shielding fraction. A similar scenario is found in cuprates and pnictides [3–5,13,14] and it may originate from magnetic and superconducting interspersed regions of nanometric size, compatible with proximity and the very short coherence length ξ of nonconventional superconductors [4]. Muons will measure a net field everywhere inside the nanoscopic mixture of M and SC regions, if these three length scales are comparable: the coherence length ξ , the mean SC domain size d and the decay distance r of the dipolar field \mathbf{B}_i from the closest M cluster (typically a few nm).

The complete phase diagram for $\text{SmFe}_{1-x}\text{Ru}_x\text{AsO}_{0.85}\text{F}_{0.15}$, obtained by combining the SQUID and the ZF- μ SR data, is shown in Fig. 3. At small Ru content a reentrant magnetic order within the FeAs layers is observed at the same $x \sim 0.10$, where T_c is dramatically reduced. Magnetic order in pnictides requires an orthorhombic structure, which has been recently demonstrated to occur [15] below 150 K already in our starting material, $\text{SmFeAsO}_{0.85}\text{F}_{0.15}$. Figure 3 shows also that, at high doping levels, both M and SC states disappear around the same threshold value $x_c \sim 0.6$, which is characteristic of magnetic interactions with nearest and next-nearest neighbors on a square lattice [16]. Notice that the same critical Ru content $x_c \approx 0.6$ is required to disrupt both superconductivity in $\text{REFe}_{1-x}\text{Ru}_x\text{AsO}_{0.85}\text{F}_{0.11}$ with $\text{RE} = \text{La}$,

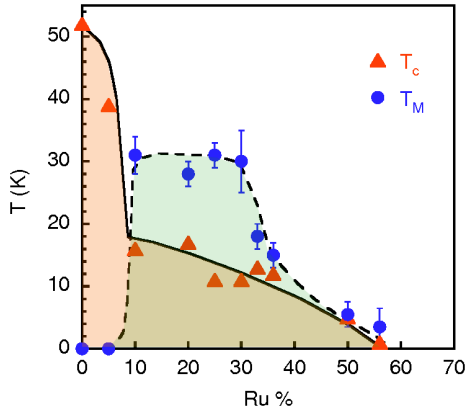


FIG. 3 (color online). (a) SQUID superconducting T_c (▲) and ZF- μ SR magnetic T_M (●) of $\text{SmFe}_{1-x}\text{Ru}_x\text{AsO}_{0.85}\text{F}_{0.15}$ vs Ru content. The lines are a guide for the eye.

Nd [10,11] and magnetic order in fluorine free $\text{REFe}_{1-x}\text{Ru}_x\text{AsO}$ with $\text{RE} = \text{La}, \text{Pr}$ [17,18]. On one hand this common critical Ru threshold emphasizes the intimate relation between magnetism and superconductivity. On the other hand the degradation of SC when M is recovered indicates a strong competition between the two respective order parameters. This apparent incongruity can be resolved by assuming that, in agreement with the most popular view, superconductivity is assisted by magnetic fluctuations. These fluctuations are suppressed by the full magnetic order, which competes with the SC state. Still short-range M order may allow fluctuations to survive alongside the M clusters, in nanoscopic form, and SC may survive as well. Upon approaching $x_c \approx 0.6$ both the static magnetism and the relevant magnetic fluctuations vanish, together with the superconductivity. Hence our results provide strong evidence for a superconductivity pairing of magnetic origin.

The presence of magnetic order in optimally F-doped RE1111 compounds was never observed before, and it is very surprising that it is induced by Ru substitution, isoelectronic to Fe and diamagnetic [8,17,18]. This scenario bears some analogies with that observed in cuprates, where the isoelectronic and diamagnetic Cu:Zn substitution recovers a frozen spin configuration, producing a concomitant sharp suppression of superconductivity [19,20].

Lang *et al.* [5] have shown that in F-doped 1111 two As local environments appear, as witnessed by two NQR peaks. They account for an intrinsic bimodal electronic inhomogeneity on a nanoscopic scale within the FeAs layers, being associated [5] to a charge-poor and a charge-rich local environment, respectively. NQR maps the local electronic configuration via the electric-field gradient at the ^{75}As nucleus and we report here how its bimodal electric-field gradient is affected by Ru substitution. In Fig. 4(a) we show the NQR spectra for representative $\text{SmFe}_{1-x}\text{Ru}_x\text{AsO}_{0.85}\text{F}_{0.15}$ samples, together with the $x = 0$ data from Ref. [5]. In addition to the double peak

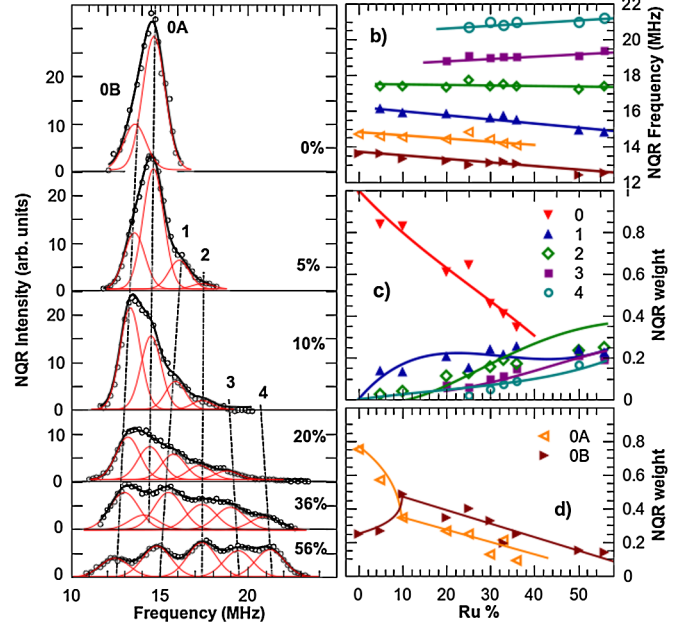


FIG. 4 (color online). (a) NQR spectra, for $T = 290$ K, with best fits and their components for selected $\text{SmFe}_{1-x}\text{Ru}_x\text{AsO}_{0.85}\text{F}_{0.15}$ samples; $x = 0$, $T_c = 52$ K, nominal F content 0.10, from Ref. [5], NQR measured at $T = 160$ K (the differences in nominal F and T are irrelevant here). (b) NQR peak frequencies vs Ru content. Lines guide the eye to identify NN Ru configurations. (c) Normalized NQR weights, a_j , $j = 0 \dots 4$ ($j = 0$ is the sum of 0A and 0B), vs Ru content, with fits (solid lines, see text). (d) Weights of 0A, 0B ($j = 0$) components.

structure (which is still visible, although much less pronounced than in F-underdoped samples [5]), up to four new satellites appear, each characterized by the number of Ru NN ions in the local fourfold coordination around As. Each spectrum has been fitted to a number of equal width Gaussian curves, varying from two to six. The five nearly equally spaced peaks of the $x = 0.56$ sample ($j = 0-4$) may be initially assigned to configurations with j Ru NN ions, respectively.

Figure 4(b) displays the best-fit central frequency of the different peaks as a function of Ru content. They can be easily grouped into six families indicated by the straight lines. Figure 4(c) displays the weight of these peaks as a function of Ru content, measured as the relative area $a_j = A_j/A_{\text{Tot}}$ ($A_{\text{Tot}} = \sum_j A_j$ is the total area), proportional to the number of ^{75}As nuclei in that environment. The $j = 0$ weight is taken as the sum of the two lower-frequency peaks, labeled 0A and 0B. Indeed Fig. 4(d) shows their separate concentration dependence, with a remarkable initial correlation: one collapses while the other grows with increasing Ru content. This suggests that they are two components of the same $j = 0$ Ru-free configuration. The assignment is supported by the good agreement of $a_j(x)$ with the fit to a binomial distribution, corrected with a weight redistribution that favors larger j , indicating a tendency towards Ru clustering [Fig. 4(c) solid lines].

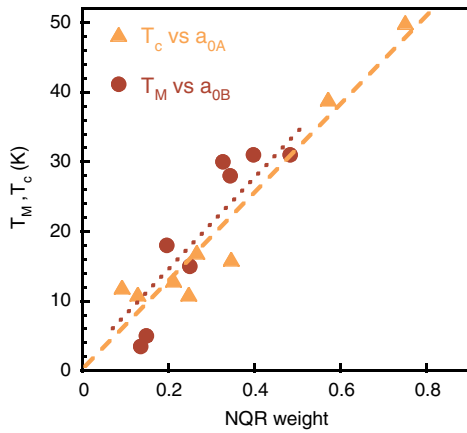


FIG. 5 (color online). T_c and T_M versus the NQR weights a_{0A} and a_{0B} respectively with their linear regressions.

The average effect of Ru substitution on the electronic properties is directly reflected in the weight of the two low frequency peaks, a_{0A} , a_{0B} , around 14.5 MHz and 13 MHz respectively, [Fig. 4(b)], representing nuclei without NN Ru ions. Comparison with the $x = 0$ spectrum in Fig. 4 clarifies that this is the same doublet already present at $x = 0$ and discussed in Ref. [5] in terms of the electronic inhomogeneity of underdoped SC. Their symmetric anti-correlated behavior for $x < 0.1$, and the clear kinks for $x \approx 0.1$ are clearly related to the change in the magnetic and superconducting properties of the system.

This is confirmed in Fig. 5, showing a nearly linear dependence of both T_c and T_M when plotted vs the NQR weights a_{0A} and a_{0B} , respectively. This correlation provides compelling evidence that the volume fraction of the charge-rich (charge-poor) local environments in the FeAs layers increases together with the strength of the average SC coupling (M coupling), i.e., the transition temperature T_c (T_M). The relation between the average coupling and the spatial extension of the ordered phase suggests a percolation transition for both orders. Given that the total charge doping is nearly constant as a function of isoelectronic Fe:Ru substitution in 1111 compounds [8,17,18], the transition must be influenced directly by a *local* charge redistribution due to Ru. The presence of Ru favors the charge-poor environment (weight a_{0B}) correlated with T_M , and causes the decrease of the charge-rich volumes (weight a_{0A}) correlated with T_c . We notice incidentally that only the $j = 0$ configuration shows the original doublet (i.e., one NN Ru ion is enough to wipe out the intrinsic electronic inhomogeneity).

In conclusion, we have shown that the isoelectronic Fe:Ru substitution in optimally F-doped $\text{SmFe}_{1-x}\text{Ru}_x\text{AsO}_{0.85}\text{F}_{0.15}$ leads to a reentrant static magnetic order which degrades the superconducting ground state. The two order parameters compete, producing a nanoscopic phase separation. The two weights, tuned by the average Ru doping, scale with the corresponding transition temperatures. Both

magnetism and superconductivity are suppressed at the percolation threshold characteristic of the magnetic system, suggesting that superconductivity cannot exist if magnetism is definitely suppressed by magnetic dilution. This picture strongly supports magnetic coupling models of superconductivity.

μSR experiments were carried out at the PSI and ISIS muon facilities. We acknowledge partial financial support from the PRIN-08 project and from PSI EU funding. Thanks are due to M. Tropeano, A. Palenzona, and C. Ferdeghini for the fruitful collaboration.

*Samuele.Sanna@unipv.it

- [1] H. Luetkens, H.-H. Klauss, R. Khasanov, A. Amato, R. Klingeler, I. Hellmann, N. Leps, A. Kondrat, C. Hess, A. Kohler, G. Behr, J. Werner, and B. Buchner, *Nature Mater.* **8**, 305 (2009).
- [2] R. Khasanov *et al.*, *Phys. Rev. B* **84**, 100501 (2011).
- [3] S. Sanna, R. De Renzi, G. Lamura, C. Ferdeghini, A. Palenzona, M. Putti, M. Tropeano, and T. Shiroka, *Phys. Rev. B* **80**, 052503 (2009).
- [4] S. Sanna, R. De Renzi, T. Shiroka, G. Lamura, G. Prando, P. Carretta, M. Putti, A. Martinelli, M.R. Cimberle, M. Tropeano, and A. Palenzona, *Phys. Rev. B* **82**, 060508(R) (2010).
- [5] G. Lang, H.-J. Grafe, D. Paar, F. Hammerath, K. Manthey, G. Behr, J. Werner, and B. Büchner, *Phys. Rev. Lett.* **104**, 097001 (2010).
- [6] J. Zhao, Q. Huang, C. de la Cruz, Shiliang Li, J. W. Lynn, Y. Chen, M. A. Green, G.F. Chen, G. Li, Z. Li, J. L. Luo, N. L. Wang, and P. Dai, *Nature Mater.* **7**, 953 (2008).
- [7] L. Boeri, O. V. Dolgov, and A. A. Golubov, *Phys. Rev. Lett.* **101**, 026403 (2008).
- [8] M. Tropeano, M. R. Cimberle, C. Ferdeghini, G. Lamura, A. Martinelli, A. Palenzona, I. Pallecchi, A. Sala, I. Sheikin, F. Bernardini, M. Monni, S. Massidda, and M. Putti, *Phys. Rev. B* **81**, 184504 (2010).
- [9] G. Allodi, S. Sanna, G. Concas, R. Caciuffo, and R. De Renzi, *Physica (Amsterdam)* **374-375B**, 221 (2006).
- [10] S. C. Lee, E. Satomi, Y. Kobayashi, and M. Sato, *J. Phys. Soc. Jpn.* **79**, 023702 (2010).
- [11] E. Satomi, S. C. Lee, Y. Kobayashi, and M. Sato, *J. Phys. Soc. Jpn.* **79**, 094702 (2010).
- [12] H. Maeter, H. Luetkens, Yu. G. Pashkevich, A. Kwadrin, R. Khasanov, A. Amato, A. A. Gusev, K. V. Lamonova, D. A. Chervinskii, R. Klingeler, C. Hess, G. Behr, B. Buchner, and H. H. Klauss, *Phys. Rev. B* **80**, 094524 (2009).
- [13] A. Keren and A. Kanigel, *Phys. Rev. B* **68**, 012507 (2003).
- [14] A. J. Drew, F. L. Pratt, T. Lancaster, S. J. Blundell, P. J. Baker, R. H. Liu, G. Wu, X. H. Chen, I. Watanabe, V. K. Malik, A. Dubroka, K. W. Kim, M. Rössle, and C. Bernhard, *Nature Mater.* **8**, 310 (2009).

- [15] A. Martinelli, A. Palenzona, M. Tropeano, M. Putti, C. Ferdeghini, G. Profeta, and E. Emerich, *Phys. Rev. Lett.* **106**, 227001 (2011).
- [16] N. Papinutto, P. Carretta, S. Gonthier, and P. Millet, *Phys. Rev. B* **71**, 174425 (2005).
- [17] M.A. McGuire, D.J. Singh, A.S. Sefat, B.C. Sales, and D. Mandrus, *J. Solid State Chem.* **182**, 2326 (2009).
- [18] P. Bonfá *et al.*, [arXiv:1110.4812](https://arxiv.org/abs/1110.4812); I. Pallecchi *et al.*, *Phys. Rev. B* **84**, 134524 (2011).
- [19] H. Alloul, J. Bobroff, M. Gabay, and P.J. Hirschfeld, *Rev. Mod. Phys.* **81**, 45 (2009).
- [20] T. Adachi, N. Oki, Risdiana, S. Yairi, Y. Koike, and I. Watanabe, *Phys. Rev. B* **78**, 134515 (2008).